Journal of Brain Science and Mental Health

PRIME OPEN ACCESS

Volume 2, Issue 1

Research Article

Date of Submission: 05 October, 2026
Date of Acceptance: 30 October, 2026
Date of Publication: 10 November, 2026

Parametric Mathematical Model for the Human's Brain Global Shape

Jérôme Chauvet*

Research and Engineering Methods For Biomathematics, Nîmes (France)

***Corresponding Author:**
Jérôme Chauvet, Research and Engineering Methods For Biomathematics, Nîmes (France).

Citation: Chauvet, J. (2026). Parametric Mathematical Model for the Human's Brain Global Shape. *J Brain Sci Ment Health, 2*(1), 01-09.

Abstract

Using two generative key components, i.e. self-similarity and sigmoid functions, we show how to build an idealized arteriovenous system that accurately encompasses the cortical hull of a human brain measured on real patient through angiographic imagery. Our algorithm, based on the constructal principle, demonstrates that, despite the complexity and sophistication of the human cerebral organ, it appears possible to gauge its general morphology by means of a theoritical model justified with pure mathematical approach and biophysical arguments. Our result might as well fit for both medical purpose and studies in evolutionary neurobiology.

Introduction

Whereas a formal algorithmic approach, namely the Lindenmayer system, has been developed for modeling the generation and design of body and organs in plants, the architectural principles of organs in mammals using abstract mathematical tools is not a common investigation approach [1-3]. A noticable recent attempt to do so was done for the human respiratory system, which was shown to benefit from a fractal architecture in order to correctly perform its physiological function [4]. However, apart from the latter, other human organs like heart, kidneys or brain, which do not exhibit an obvious tree-like structure, did not become the logical follow-ups of equivalent studies.

The human brain is considered the most complex organ in human anatomy because of its many connections throughout the body between the central nervous system and all external sensory-motor systems, so that its structure is abondantly studied part by part, from cells to functional areas, aiming at determining mutual dependencies between functional identified sub-systems [5-7]. Meanwhile, through embryogenesis all organs of the human anatomy must grow harmoniously with respect to a constructive global process driven by genes from simpler to more complex structures [8,9]. for which we can still nowadays question about the way to model them within a theoritical frame using generative functions and computation. Some fundamental principles for the cerebral function are recognized to be essential. On top of the list, since the brain does not store biochemical energy locally as glycogen or triglycerids, but consumes a lot continuously, it should be provided with both glucose and oxygen on a regular basis directly from the blood through current access to blood flow, which thus must be privileged by maximizing this access for brain cells, especially neurons. In that sense, hypoglycemia due to diabetes is known to cause mental troubles with loss of awareness and rapid fainting [10]. Furthermore, the tight control of incoming substances into the brain tissue (neurons and glial cells) by the Blood-Brain Barrier (BBB) is another strong argument advocating for a brain global architecture favoring blood supply efficiency placed at the center of the generative view of it [11]. According to this idea, monitoring control of blood flow within the brain in order to understand the cerebral function is the basic concept of functional magnetic resonance imaging [12].

The so-called constructal design approach states that an engineered system, which has to deal with a continuous flow of substances (heat, matter, information) streaming through itself must adapt to this traversing flow as a fractal structure in order to reduce resistance against it, and so facilitate global ubiquitous distribution whilst preventing itself from rapid entropic decay [13]. This is known to be the basic principle for a tree dealing with flowing sap systems and we are led to question how the human brain might resort to the same logic into resolving its own functional purpose [14].

In this article, taking the constructal principle as a foundational algorithm for the brain's vasculature, we develop a mathematical method able to generate realistic computed models of the human's brain geometry. This constitutes a novel theory accounting for the global shape and properties of the human brain relating geometrical features caraterized by size-to-size ratios to a clear-cut modular organization of the cerebral volume.

Material and Methods

The constructal principle takes in reversed logic the fractal geometry paradigm, which characterizes shapes and forms through self-similarity up to possibly infinite recursions inwards and outwards of the same basic pattern. As a design method for engineering a flowing system, a basic pattern must be identified that responds to special constraints with regard to the traversing flow. Through recursive iteration, rescaling and auto-connections of this first element, the needed property must deploy throughout countless ramifications up to a calculable limit.

In order to reproduce the basic theoritical pattern of a vascular tree within human tissues, we consider the parametric fork as the very first element of any blood circulatory system (Figure 1). This basic pattern is made of two continuous sigmoid functions smoothly dispatching one initial stream of blood into two halves without either asymmetrical disruption or rough turn.

Sigmoid functions are a large family of functions all characterized by a S-like form : we chose those that allow rapid computation and fulfill the requirement of driving a path from negative infinity to positive infinity with a gentle splitting trajectory [15]. The blood flow is considered through the use of parameter u as the common value passed to a symmetric couple of instances mirrored by the base stream line. For this study, we identified two candidates functions, namely the arctangent and erf, for comparison. As shown in Figure 1, when adjusted to each other the two candidates functions differ by a certain level of added torsion especially for the arctangent.

The following shows the result after generating a parametric tree out of the latter. The bundle function $\vec{B}(u)$ is a set of 2^D single paths $H_i(u)$, Dbeing the depth of the bundle.

Whilst u has a space and/or temporal value, i.e. along with the flow, $H(u)$ translates spatial displacement apart from the initial flow line, which is implicitely oriented either for dichotomic distribution or for contra-dichotomic gathering of the blood content.

$$h_{ij}(u) = S_{ij} A_{ij} \sigma(\Omega(u - \varphi_{ij}))$$

$$\text{with } \sigma(x) = \frac{1}{\pi}\arctan(x) + \frac{1}{2}$$

$$H_i(u) = \sum_{j=0}^{D-1} h_{ij}(u)$$

$$\varphi_{ij} = (i+1)\Delta_u$$

$$\vec{B}(u) = (H_0(u), H_1(u), \ldots, H_{2^D-1}(u))$$

$$A_{ij} = \frac{1}{2^{D-i-1}}$$

$$S_{ij} = \begin{cases} (-1)^j & i = 0 \\ S_{0\lfloor j/2 \rfloor} & i > 0 \end{cases}$$

ϕ controls the distance between two successive forks along each single path, defined with regular spacing Δ_u. A is the amplitude factor affecting the displacement after each splitting node, divided by two everytime the number of paths doubles. S stands for "sign" and equals to either 1 or -1 so as to define the next direction of a single path after every node. The Ω factor controls the steepness of splitting paths, i.e. softer with lower values and edgier with higher values. All in all, this generative model represents an idealised walking process for vasculogenesis without randomized behavior.

The following piece of code shows how function $\vec{B}(u)$, the so-called bundle function, should be implemented after defining the depth of the tree D and choosing a standard value Ω for the whole bundle stored in a table W.

```
/* GENERATE TREE STRUCTURE */
for(int k = 0; k < D; k++) {
  for(int n = 0; n < pow(2,D) ; n++) {
    W[k][n] = -1;
    A[k][n] = 1/pow(2,D-k-1) ;
    phi[k][n] = (k+1)*4;
```

```
  }
}

S[0][0] = 1;
for(int n = 1; n < pow(2,D) ; n++) {
  S[0][n] = 1 - S[0][n - 1];
}

for(int k = 1; k < D; k++) {
  for(int n = 0; n < pow(2,D) ; n++) {
    S[k][n] = S[0][floor(n/pow(2,k))];
  }
}

for(int k = 0; k < D; k++) {
  for(int n = 0; n < pow(2,D) ; n++) {
    S[k][n] = S[k][n] - 1 ;
  }
}
```

For a sigmoid function chosen to be arctangent, the following loop stores the trajectories of the 2^D paths within a table for which the total number of intermediate steps has been previously defined.

```
/* COMPUTE BUNDLE FUNCTION INTO A BIDIMENSIONAL TABLE */
if(ReCalc==true){
    for (int i = 0; i < u_max; i++) {
      for (int n = 0; n < pow(2,D); n++) {
        Add = 0;
        for (int j = 0; j < D; j++) {
        Add = Add + S[j][n]*A[j][n]*(atan(W[j][n]*(t - phi[j][n]))/PI+0.5);
        }
        Bundle[n][i]  = Add;
      }
      u = u + du;
    }
  ReCalc = false;
}
```

This algorithm has no tricky part except when depth factor D exceeds a certain value since $2^D \times u_{max}$ values will in turn be generated and stored.

Taken as a guiding function, Figure 2 demonstrates the possibility to use the bundle function to generate the geometrical equivalent of an arterial, resp. venous, fork element of an abstract vascular system [16,17]. This model relies on a voxel space having two possible states per voxel, either full or empty [18]. The parametric fork function serves for determination of the progressive distance between separating sub-vessels. The whole three dimensional fork structure is generated slice by slice following progress of parameter u whilst vessel walls are defined by full voxels in the neighbourhood of empty ones. Full voxels are chosen according to the calculation of a couple of metaballs added and displaced within each slice according to the following formula [19].

$$\rho(x,y) = \Theta\left(\frac{1}{\delta((F\sigma(u), h/2), (x,y))} + \frac{1}{\delta((-F\sigma(u), h/2), (x,y))}\right) = 0 \text{ or } 1$$

where, for the k^{th} bidimensional slice defined as $u = k\Delta$ (Δ being the physical length of a slice), F defines the width of the current forking distance, h the height of the slice, x and y the position within the current slice. Greek letters are the

functions : the sigma function σ for the trajectory, δ the distance between two points within the current slice, and ρ yields a density level at point (x,y) comprised between 0 and 1 whilst Θ represents a threshold function defining whether a voxel at (x,y) is full (1) or empty (0) given the value of the input passed to it between zero and infinity .

Considering the basic fork in Figure 1, the following piece of code generates the result shown in figure 2B based on the formula above. A voxel space, here named a voxel slice, must be defined as a bidimensional table with previously defined width and height (here 120x50 voxels). Threshold values 0.08 and 0.12 define how thick the walls of vessels must be and can be tested for experimental validation.

```
/* GENERATE VASCULOGENESIS MODEL */
for(int u = 0 ; u < u_max ; u++){
  /* CALCULATE FORK FUNCTION */
  LeftPath_X = 60 - 25*atan(-0.06*u+1) + 15;
  RightPath_X = 60 + 25*atan(-0.06*u+1) - 15;

  for(int i=0 ; i < VxlSpc_Wdth ; i++){
    for(int j=0 ; j < Vxlspc_Hght ; j++){

      /* COMPUTE EUCLIDEAN DISTANCE BETWEEN EACH VOXEL AND BOTH PATHS */
      float Dist_Left = sqrt((i-LeftPath_X)*(i-LeftPath_X)
                             +(j-Pos_Y)*(j-Pos_Y));
      float Dist_Right = sqrt((i-RightPath_X)*(i-RightPath_X)
                              +(j-Pos_Y)*(j-Pos_Y));

      /* COMPUTE PLANAR METABALLS WITHIN VOXELSLICE */
      VoxelSlice[i][j] = 1/Dist_Left + 1/Dist_Right;

      if(VoxelSlice[i][j] < 0.08 || VoxelSlice[i][j] > 0.12){
        VoxelSlice[i][j] = 0;
      }
      else{
        VoxelSlice[i][j] = 1;
      }
  }
```

Interestingly, the mere arithmetic addition of two constant metaballs withing the scalar field of a single slice suffices to generate both a smooth branching and a proper narrowing of the two daughter-vessels diameter after splitting, like expected with the Murray's rule [20]. In Figure 2 also (on the right), we show that the parametric bundle can be mapped onto a surface that admits a bidimensional parameterization. As such, the Moebius strip is an instance of bidimensional surface with both constant torsion and cycling global structure, which reflects in mathematical form the need in anatomical context for elasticity of the blood circulatory system. This system is an abstract vasculature using four times the bundle function so as to build an arteriovenous basic loop circuitry (red for arteries, blue for veins) virtually distributing firstly oxygenated blood (from red to blue) to a set of single sites (possibly little groups of cells), then refreshing the blood in a second part of the cycle (from blue to red) according to the respiratory function. This construct should be generated like the following shows

```
/* BUILD MINIMAL PARAMETRIC CIRCULATORY SYSTEM AS SUPER-BUNDLE FUNCTION */
float[][] SuperBundle = new float[floor(pow(2,D))][4*t_max+1];
float[] BloodColor = new float[4*t_max+1];

for (int i = 0; i < t_max; i++) {
  for(int n = 0; n < pow(2,D) ; n++) {
     SuperBundle[n][t_max-i]=Bundle[n][i];
     SuperBundle[n][t_max+i]=Bundle[n][i];
```

```
        SuperBundle[n][t_max-i+2*t_max]=Bundle[n][i];
        SuperBundle[n][t_max+i+2*t_max]=Bundle[n][i];

    }
    BloodColor[i]=255;
    BloodColor[i+t_max]=0;
    BloodColor[i+2*t_max]=0;
    BloodColor[i+3*t_max]=255;
}
```

Although appearing intuitively synthetic-looking and somewhat much too regular to fit with natural organic structures, we investigated accordance of our generative model with real instances of brain circulatory blood meshes. Figure 3 shows how a proper fit can be realized between real 7T MRI cerebral scans and our generative model. In this clinical instance, an adult patient has been submitted to a cerebral angiographic scan so that each scan is an image of a projection along one of the three spatial axis. We superposed over these planar measurements couples of bundle functions facing each other to reproduce the arteriovenous interweaving logic, looking for the best stretch manually. For the top view, we also made it using optic photographs of brains extracted from human corpses with the same level of accuracy (data not shown).

Our method reveals that the overall architecture of the human brain, the underlying hull structure, has universal proportions defined by exact numeric ratios. Given the 8 parts shown in Figure 3 (frontal superior, frontal inferior, parietal, occipital, right or left everytime), we have identified the following rules

- Bilateral symmetry between left and right brain defines a trivial ratio of 1/1 = 1
- Lengths ratio along antero-posterior axis between frontal and parietal parts is 3/2
- Heights ratio along longitudinal axis between occipital part and parietal part is 1/2
- Inferior frontal and superior frontal parts also have a distinguished ratio of 3/4

Figure 3 also shows how these theoritical ratios affect in parallel the cerebral standard volume for the human adult anatomy. We define a XYZ reference frame built out of these ratios, i.e. an unconventional orthonormal basis with origin separating eight regions (volume cuts) for which anterior and posterior (superior and inferior respectively) have opposite orientations with different base norms. As shown here, the theoritical cranial dome can be modeled directly from these eight vectors taken as a basis used to stretch accordingly quarters of arches provided by the generic cartesian function of ellipsoids. More precisely in Figure 4, we mathematically define the precise values needed for this cartesian volume, within which the cerebral arteriovenous vascular trees are laid, to fit perfectly with the cerebral content (and the cortex in particular). Hence, both the human cerebral organ and its protective shell, namely the cranial bone, appear to share the same numeric rules defining their proportions in modular elements.

Discussion

This experimental result and our theoritical construct meet over the requirement of determining the design principles underlying the shape of the human brain. Although the approach could be wildly criticized for mimicking in a plastic-like form natural structures far more complex and intricate than pure mathematical objects, the theory proves to be relevant and should be better understood as a profound insight into the underlying plan, which a biological system like the human brain must stick to to perform its complex function. Since the human brain is thought to be one of the most complex organs amongts all living organisms, it would appear more objectively astonishing to state its structure should have no exact design principles to be discovered. The theory provides a novel way to work on an idealized model for the human brain and to perform in silico manipulations and experimental validations. The identification of size-to-size exact ratios involving progressive fractional numbers (1/2, 2/3, 3/4) parallels in an unexpected but coherent way the phylogenetic statement that evolution has developed frontal structures and functions lately in species history into bigger structures so as to fulfill more complex tasks like social organisations, interactions and world representation. This corresponds to the frontal cortical extension being three times as long as the occipital height and twice as long as the parietal part.

Geometrically speaking, exact ratios often show up in theories based on the constructal principal since these values yield certain distributive properties with regard to essential physical values. As per the Murray's law for the vascular subdivision rule, length-to-area and area-to-volume size preservation help distributive systems adapt their shape to spatial constraints by involving in their geometry dimensions as architectural features [21]. It is also noteworthy that the tree-like vascular structures forming the cerebral internal mesh for in-and-out blood supply and the Cartesian modelization of the cranium around them can adapt to each other in a harmonious way. Essentially, the main function of the cranial bone is to protect the brain from physical traumas : its typical dome-shaped architecture allows for better energy dissipation in case of physical shocks whilst protecting the inside.

Meanwhile, the mathematical parameterization based on the arctangent function for the vascular trees together with Cartesian ellipsoidal functions for the dome lead to natural solutions that resolve perfect fit of the one to the other. This intelligent combination of geometric properties in two different organic tissues (brain and cranium) is obviously a key anatomic feature to species survival and appears here born from pure mathematical characteristics without consideration of cellular or biochemical special properties.

Clinically speaking, this theory might also provide an enhanced gauging method for assessing normal brain development in embryos and infants as long as imagery can give access to these ratios. Further clinical observations and comparisons using the idealized model provided by these ratios with patients suffering from microcephaly for example should give more quantitative insight into the link between brain geometry and the specification of certain neurological syndrome, possibly also based on parental characteristics [22,23]. All in all, this mathematical approach adds up to the many recent attempts to comprehend the cerebral structures in bottom-up approach (from cells to global structure), i.e. focusing on neuronal physiology and wiring description, whilst ours proves relevant as a top-down way (from general principles to detailed single elements) to comprehend the organ functioning rather as an engineered system adapting to its physical context. Accordingly, the theory might also prove very helpful in studies aiming at characterizing the anatomical evolution of the central nervous system amongst species [24].

Acknowledgements

The author would like to thank Dr. Erik Middlebrooks of Mayo Clinic Florida for providing the relevant clinical data. Also, Dr. Olivier Martinez of Université Paul Sabatier and Dr. Daniel Tomé for pointing out the interest of this result during a first presentation to my professional network.

Additional Review Material

Generator of Y-shaped branching using B function in voxel space : https://youtu.be/iBEFvCIS49U
Mapping of a basic circulatory system onto Möbius strip : https://youtu.be/zrZjCmOAilo
The hull generator written in Processing 4.3 : https://github.com/SewuJC/brain-envlp-generator

References

1. Lindenmayer, A. (1986, October). Models for multicellular development: Characterization, inference and complexity of L-systems. In International Meeting of Young Computer Scientists (pp. 138-168). Berlin, Heidelberg: Springer Berlin Heidelberg.
2. Lindenmayer, A., & Jürgensen, H. (1992). Grammars of development: discrete-state models for growth, differentiation, and gene expression in modular organisms. In Lindenmayer systems: Impacts on theoretical computer science, computer graphics, and developmental biology (pp. 3-21). Berlin, Heidelberg: Springer Berlin Heidelberg.
3. Lindenmayer, A., & Prusinkiewicz, P. (2019). Developmental models of multicellular organisms: A computer graphics perspective. In Artificial life (pp. 221-249). Routledge.
4. Ionescu, C., Oustaloup, A., Levron, F., & De Keyser, R. (2009). A model of the lungs based on fractal geometrical and structural properties, accepted contribution at the 15th IFAC Symposium on System Identification, St. Malo, France, 6(9).
5. Hayden, B. Y., Heilbronner, S. R., & Yoo, S. B. M. (2026). Rethinking the centrality of brain areas in understanding functional organization. Nature Neuroscience, 29(2), 267-278.
6. Dorkenwald, S., Matsliah, A., Sterling, A. R., Schlegel, P., Yu, S. C., McKellar, C. E., ... & Murthy, M. (2024). Neuronal wiring diagram of an adult brain. Nature, 634(8032), 124-138.
7. Maier-Hein, K. H., Neher, P. F., Houde, J. C., Côté, M. A., Garyfallidis, E., Zhong, J., ... & Descoteaux, M. (2017). The challenge of mapping the human connectome based on diffusion tractography. Nat Commun 8: 1349.
8. Yang, Runhua, Fen Ji, and Jianwei Jiao. "Early central nervous system development and neuron regeneration." Current Opinion in Genetics & Development 90 (2025): 102286.
9. Lawrence, J. E., Roberts, K., Tuck, E., Li, T., Mamanova, L., Balogh, P., ... & Behjati, S. (2024). HOX gene expression in the developing human spine. Nature communications, 15(1), 10023.
10. Nimgampalle, M., Chakravarthy, H., & Devanathan, V. (2021). Glucose metabolism in the brain: An update. In Recent developments in applied microbiology and biochemistry (pp. 77-88). Academic Press.
11. Wu, D., Chen, Q., Chen, X., Han, F., Chen, Z., & Wang, Y. (2023). The blood–brain barrier: Structure, regulation and drug delivery. Signal transduction and targeted therapy, 8(1), 217.
12. Leskinen, S., Singha, S., Mehta, N. H., Quelle, M., Shah, H. A., & D'Amico, R. S. (2024). Applications of functional magnetic resonance imaging to the study of functional connectivity and activation in neurological disease: A scoping review of the literature. World Neurosurgery, 189, 185-192.
13. Bejan, A. (2000). Shape and structure, from engineering to nature. Cambridge university press.
14. Lorente, S., & Bejan, A. (2006). Heterogeneous porous media as multiscale structures for maximum flow access. Journal of applied physics, 100(11).
15. https://en.wikipedia.org/wiki/Sigmoid_function
16. Andrejecsk, J. W., & Hughes, C. C. (2018). Engineering perfused microvascular networks into microphysiological systems platforms. Current Opinion in Biomedical Engineering, 5, 74-81.
17. Vailhé, B., Vittet, D., & Feige, J. J. (2001). In vitro models of vasculogenesis and angiogenesis. Laboratory investigation, 81(4), 439-452.

18. Foley, J. D. (1996). Computer graphics: principles and practice (Vol. 12110). Addison-Wesley Professional.
19. https://en.wikipedia.org/wiki/Metaballs
20. Smink, J. S., Hagmeijer, R., Venner, C. H., & Visser, C. W. (2025). Optimising branched fluidic networks: a unifying approach including laminar and turbulent flows, rough walls and non-Newtonian fluids. Journal of Fluid Mechanics, 1011, A42.
21. Wang, K. M., Lorente, S., & Bejan, A. (2010). Vascular structures for volumetric cooling and mechanical strength. Journal of Applied Physics, 107(4).
22. Gilmore, J. H., Knickmeyer, R. C., & Gao, W. (2018). Imaging structural and functional brain development in early childhood. Nature reviews neuroscience, 19(3), 123-137.
23. Pritschet, L., Taylor, C. M., Cossio, D., Faskowitz, J., Santander, T., Handwerker, D. A., ... & Jacobs, E. G. (2024). Neuroanatomical changes observed over the course of a human pregnancy. Nature Neuroscience, 27(11), 2253-2260.
24. Northcutt, R. G. (2012). Evolution of centralized nervous systems: two schools of evolutionary thought. Proceedings of the National Academy of Sciences, 109(supplement_1), 10626-10633.

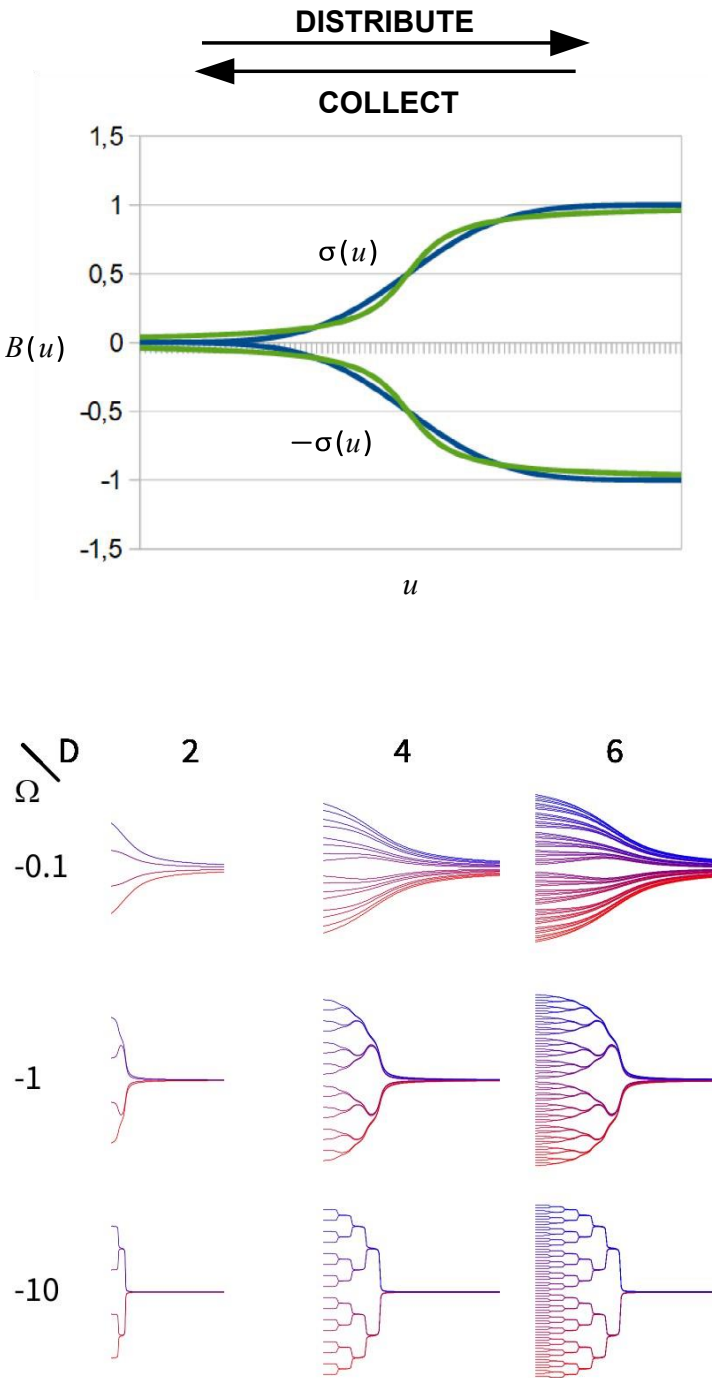


Figure 1: Vascular Bundle as a Self-Similar Constructal Tree

Above : comparison of two candidates for the sigmoidal fork, i.e. erf (blue) and arctan (green) as generative function. Below : computation of the vessels bundle function with arctangent using different values for depth D and Ω control parameters.

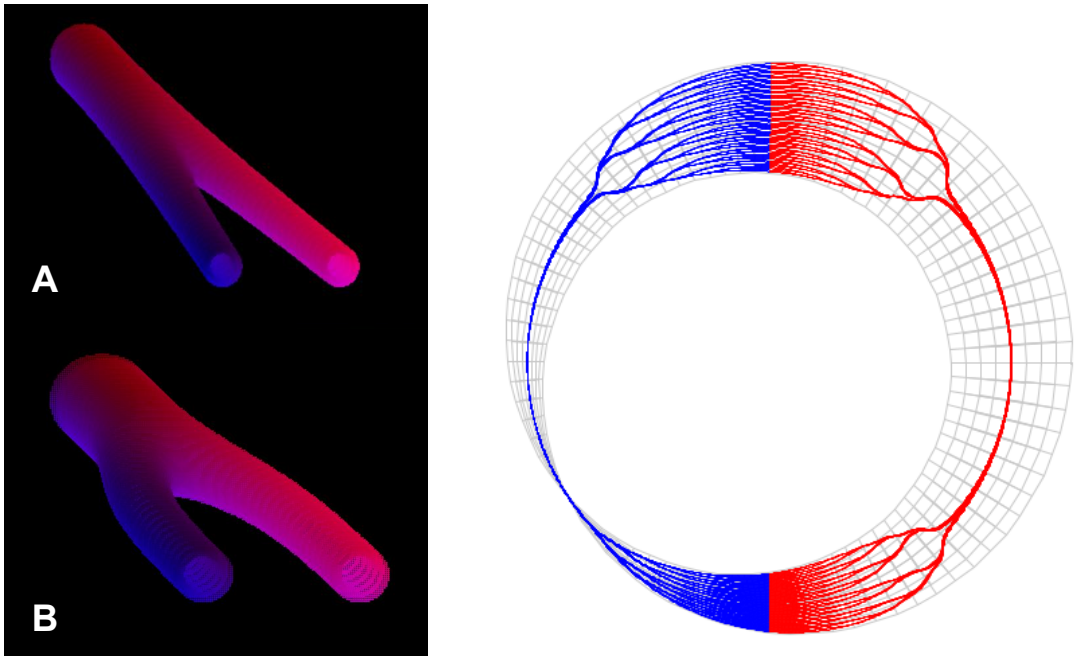


Figure 2: Generation of Anatomic Structures

Left : (A) linear versus (B) guided by the bundle function branching of vessels in a voxelspace. Right : parametric feature allows to map a basic circulatory mesh on a Moebius strip with an arterial part (red) connected to a veinous part (blue).

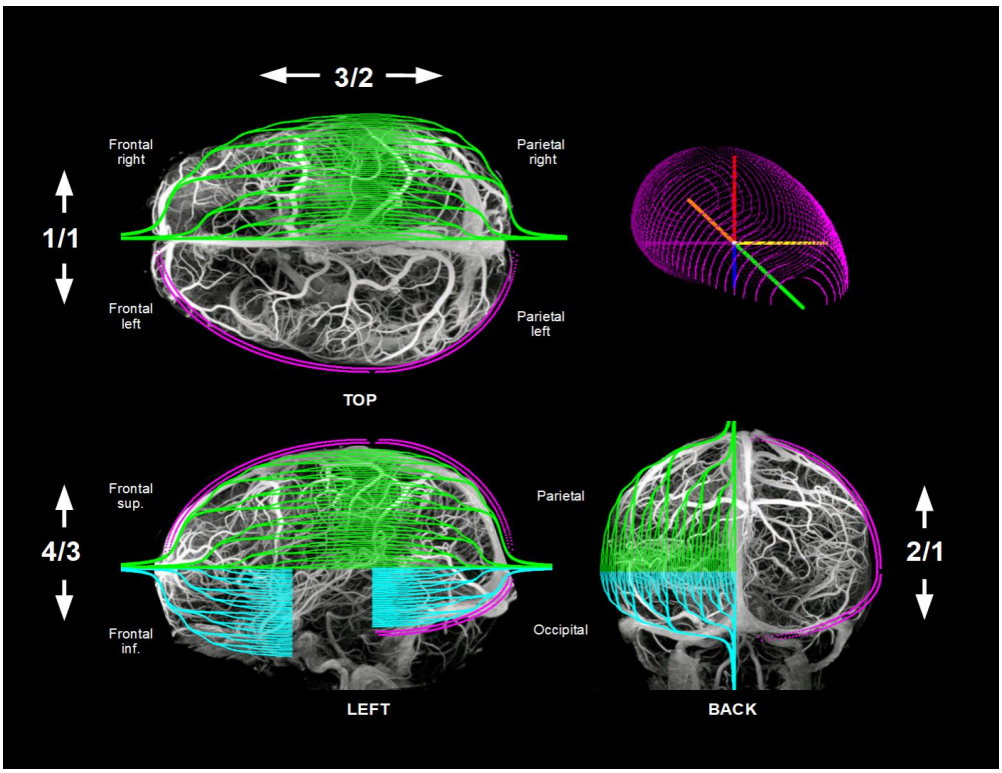


Figure 3: Best Fit to Angiographic Data

Real instance of human brain vasculature compared with the bundle function (green+cyan) and shell function (pink). Ratios indicate the stretch factor needed to pass from one part to the other according to arrows. Best fit is obtained with control parameters (D, Ω) = (6, -1).

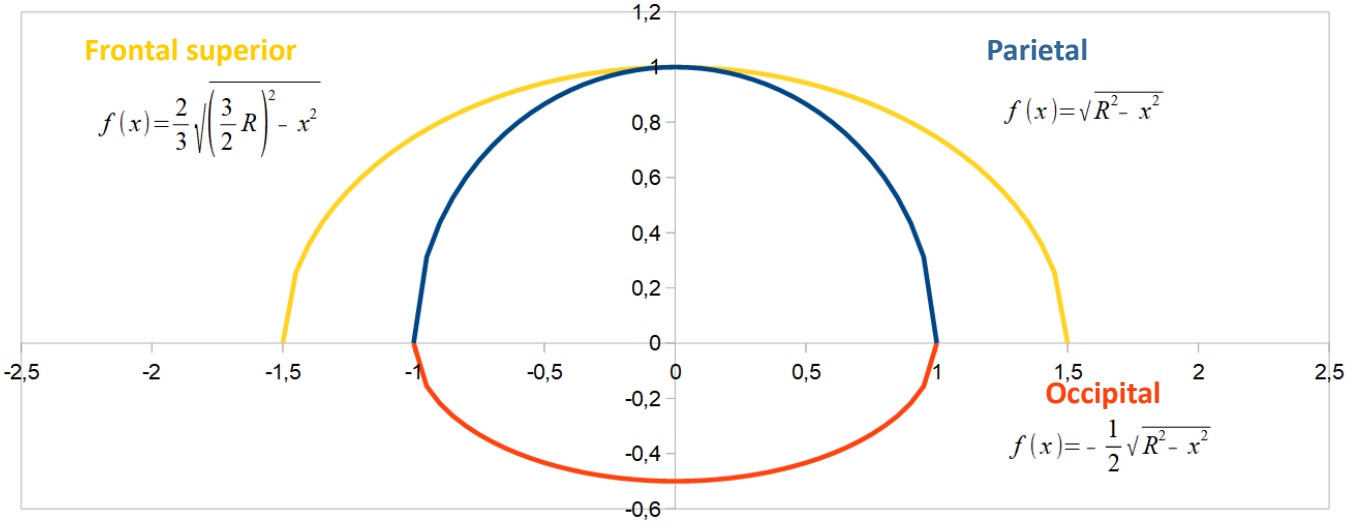


Figure 4: Modelisation of the Cranial Dome with Cartesian Functions

Radius R is made equal to 1 and can be determined for a real cranium with sagittal length L according to L = 2/5 R.